Polymer Degradation and Stability 204 (2022) 110096

Contents lists available at ScienceDirect

Polymer Degradation and Stability

journal homepage: www.journals.elsevier.com/polymer-degradation-and-stability

Detecting, characterising and assessing PEEK's and CF-PEEK's thermal degradation in rapid high-temperature processing

Dimitrios Gaitanelis [a,b,*], Chris Worrall [c], Mihalis Kazilas [d]

[a] Department of Mechanical and Aerospace Engineering, Brunel University London, London, Uxbridge UB8 3PH, United Kingdom
[b] NSIRC, TWI Ltd, Granta Park, Great Abington, Cambridge, CB21 6AL, United Kingdom
[c] Advanced Composites and Adhesives Section (ACA), TWI Ltd, Cambridge, CB21 6AL, United Kingdom
[d] Brunel Composites Centre (BCC), Brunel University London, London, Uxbridge UB8 3PH, United Kingdom

ARTICLE INFO

Keywords:
Poly-ether-ether-ketone (PEEK)
Carbon fibre (CF)
Thermo-oxidative degradation
Fast heating rates
Infrared (IR) spectroscopy
Differential scanning calorimetry (DSC)

ABSTRACT

In this study, a methodology is proposed that can identify and characterise the extent of thermal degradation that takes place in rapid high-temperature processing of PEEK and CF-PEEK. Initially, their decomposition mechanisms are examined in air with thermogravimetric analysis (TGA). Then, PEEK and CF-PEEK samples are heated in static air conditions up to temperatures that are close to and above the onset of thermal degradation with heating rates up to 100 °C/min. The samples are then examined with attenuated total reflection - Fourier transform infrared (ATR-FTIR) spectroscopy and a new fluorenone peak is detected at 1711 cm^{-1} that is directly linked with the progress of degradation. A correlation between its intensity and the resulting thermal degradation takes place and it is shown that the 1711 cm^{-1} peak can be safely used as a tool for characterising the extent of thermal degradation at the examined heating conditions. Finally, an investigation with differential scanning calorimetry (DSC) is conducted to identify the extent of thermal degradation that would not induce a severe thermal damage on the two materials. In both PEEK and CF-PEEK, faster heating rates are found to have a reduced effect on their crystallinity content and a degradation around 1% of their PEEK matrix content is found tolerable.

1. Introduction

Poly-ether-ether-ketone (PEEK) is a semi-crystalline polymer with good mechanical properties and a desirable combination of high chemical resistance and thermal stability [1]. It was firstly produced by DuPont laboratories and Imperial Chemical Industries (ICI) in the early 1960s [2] and comparing to other polymers, it has an enhanced thermal degradation resistance due to the stable aromatic backbone that comprises the bulk of its monomer unit [3]. Moreover, with a continuous use temperature of 270 °C and a melting point around 343 °C [4], PEEK is commonly used as a polymer matrix in applications where high temperatures are applied. In addition, its carbon fibre (CF) reinforced composites have a significantly high stiffness to weight ratio that makes them an ideal candidate for replacing metallic elements in the aerospace industry [5]. As a matter of fact, CF-PEEK composites can be found in several structures of an aircraft such as access panels, floor panels and wing flaps [6]. Furthermore, CF-PEEK's excellent thermal and chemical properties have made it a strong candidate for applications where harsh thermo-chemical environments exist such as the region close to the aircraft engine [7]. Therefore, an important amount of ongoing research currently focuses on the response of PEEK and CF-PEEK at high temperatures and oxidative environments and investigates their thermo-oxidative degradation mechanisms [1,7–10].

Most of the studies that have examined PEEK's and CF-PEEK's response to these conditions have focused on the degradation of the material after long-time heating [3,7,9,11,12]. A number of studies have examined PEEK's degradation in short processing cycles (<5 min) [1,10,13] and a few studies have also examined CF-PEEK's degradation in the conditions experienced in laser-assisted tape placement (LATP) [8,14] and laser heating [15]. Considering PEEK's and CF-PEEK's wide application in processes where rapid high-temperature processing is applied, it is important to further examine their response in these conditions.

Overall, PEEK and CF-PEEK can be reworked and reprocessed at temperatures around 400 °C and an even further temperature increase locally (e.g. with laser heating) can lead to even faster processing cycles [1,15]. One of the issues that can arise when PEEK and CF-PEEK are

* Corresponding author at: Department of Mechanical and Aerospace Engineering, Brunel University London, London, Uxbridge UB8 3PH, United Kingdom.
E-mail address: dimitrios.gaitanelis@brunel.ac.uk (D. Gaitanelis).

https://doi.org/10.1016/j.polymdegradstab.2022.110096
Received 22 June 2022; Received in revised form 30 July 2022; Accepted 4 August 2022
Available online 6 August 2022

processed with rapid high-temperature processing is the activation of their degradation mechanisms. Thermal degradation initially induces a rapid viscosity increase that can impact the processability of the materials [16,17]. At higher temperatures, the viscosity increase is followed by weight loss due to thermal degradation. This can affect PEEK's and CF-PEEK's post-processing integrity by deteriorating their mechanical properties and by reducing their service time [8,15]. As a matter of fact, thermal degradation has been identified as one of the main damage mechanisms in several applications of composites where rapid high-temperature processing is applied such as induction welding [18,19], composite-metal laser joining [20–23] and composites machining [24–28].

The two main parameters that affect PEEK's and CF-PEEK's thermal degradation in these applications are the reached temperatures and the dwell time at these temperatures [8]. When fast heating is applied though, the exact combination of reached temperatures and dwell time that would not induce a thermal damage on the materials is not easily defined and has not been extensively studied yet. However, considering that thermal degradation is a significant damage mechanism in several applications of PEEK and CF-PEEK, it is important to be able to detect its occurrence after applying rapid high-temperature processing. Therefore, in this study a methodology is proposed that can detect the event of thermal degradation in PEEK and CF-PEEK and it can also characterise its extent in rapid high-temperature processing.

Initially, PEEK's and CF-PEEK's decomposition is examined with thermogravimetric analysis (TGA) in an air atmosphere with heating rates up to 100 °C/min and the main degradation mechanisms that take place are highlighted. Then, PEEK and CF-PEEK samples are heated with 5, 20, 50 and 100 °C/min up to temperatures that are below the onset of degradation and temperatures that result up to a maximum mass loss of 15% and 6.7% respectively. The partially degraded samples are then examined with attenuated total reflection - Fourier transform infrared (ATR-FTIR) spectroscopy and a new peak is detected at 1711 cm^{-1} that is directly linked with the process of degradation. It is shown that the intensity of the 1711 cm^{-1} peak can be used as a valid tool for detecting and characterising the extent of thermal degradation that takes place in both PEEK and CF-PEEK after a heating process where rapid high-temperature processing is applied. In addition, to assess the effect of the thermally induced damage on the crystallinity content of the two materials the thermally degraded samples are examined with differential scanning calorimetry (DSC). Through this process, the extent of thermal degradation that does not significantly affect the degree of crystallinity (DOC) of PEEK and CF-PEEK is identified in an attempt to further define the materials' thermal limits in rapid high-temperature processing. In both the materials, a degradation around 1% of their PEEK content is found tolerable and does not impact their DOC. Finally, the effect of the applied heating rate is also assessed and it is shown that faster heating rates affect the DOC of PEEK and CF-PEEK to a lesser extent.

2. Materials and methods

2.1. Materials

The PEEK samples are provided by Engineering & Design Plastics Ltd., Cambridge, UK and have a density equal to 1.3g/cm^3 and a glass transition temperature (T_g) equal to 145 °C ± 0.7 °C. After a DSC assessment, the material's initial crystallinity content is equal to 43.7% ± 0.4% and its melting point (T_m) is found at 342.7 °C ± 1.8 °C. The CF-PEEK samples are obtained from a CF-PEEK laminate produced at TWI Ltd., Cambridge, UK. The bulk laminate was manufactured with thermoplastic unidirectional (TPUD) prepregs provided by Teijin Limited. These prepregs (Tenax® -E TPUD PEEK-HTS45) have a PEEK matrix content of 34% of the overall weight and utilise Tenax®-E HTS45 CFs [29]. From the DSC investigation, the reinforced material was found to have a T_g equal to 140.3 ± 0.8 °C, a T_m around 340.3 °C ± 0.2 °C and a DOC equal to 34.7% ± 0.6%.

2.2. Methods

Various heating programs are applied to examine the response of PEEK and CF-PEEK in slower and faster high-temperature processing. Initially, PEEK's and CF-PEEK's degradation mechanisms are examined with TGA in a 50 ml/min airflow with heating rates up to 100 °C/min. Then, PEEK and CF-PEEK samples are heated in static air conditions with several heating rates up to temperatures close to and above the onset of thermal degradation. In particular, samples are heated up to temperatures between 460 °C and 600 °C with heating rates of 5, 20, 50 and 100 °C/min. To identify the resulting level of degradation, the mass of each sample is measured before and after the applied heating programs. Then, the partially degraded samples are examined with ATR-FTIR and DSC.

2.2.1. TGA

The thermal degradation of PEEK and CF-PEEK is initially examined with TGA in an air atmosphere. The examined PEEK samples have an initial mass of 7.6 ± 0.6 mg and the examined CF-PEEK samples have an initial mass of 7.2 ± 1 mg. A calibrated TGA 2 thermogravimetry from Mettler Toledo is used and initially an isothermal segment at 30 °C is applied in each heating program for 10 min. Then, each sample is heated in an airflow of 50 ml/min up to a maximum of 1130 °C with an applied heating rate of 5, 20, 50 and 100 °C/min.

2.2.2. ATR-FTIR

In this study, a Nicolet iS50 FTIR spectrometer operating with the built-in diamond ATR from Thermo Fischer Scientific Inc. is used and the accumulated spectra are post-processed in OriginLab® software. All the spectra are collected from 4000 to 600 cm^{-1} with a resolution of 4 cm^{-1} and a total of 128 scans. Three samples are examined for each heating program and five different measurements take place for each sample. In general, ATR-FTIR spectroscopy can detect the changes of the molecular structure that occur in the material's surface and is a useful technique for following the spectral changes that occur in PEEK and CF-PEEK upon thermal degradation [15]. However, the intensity of the spectra in each measurement depends on the contact area between the specimen and the prism, which can vary between different measurements. Therefore, further processing is required to ensure the physical significance of the accumulated spectra in the molecular level [30]. Hence, to proceed to a valid comparative study the accumulated spectra are baseline-corrected and normalised to one distinct peak. In our study, the phenyl ring stretching peak at 1593 cm^{-1} was the strongest upon degradation and is therefore used as the normalisation reference.

2.2.3. DSC

The PEEK and CF-PEEK samples that have been partially degraded in static air conditions with the four examined heating rates are then run in a DSC device (Perkin Elmer DSC 4000) according to the following program:

- 20 °C - 360 °C with a heating rate of 10 °C/min (hold for 10 min);
- 360 °C - 20 °C with a cooling rate of 10 °C/min (hold for 10 min);
- 20 °C - 400 °C with a heating rate of 10 °C/min.

The heat-cool-heat analysis takes place in a nitrogen atmosphere (20 ml/min) and the examined partially degraded PEEK and CF-PEEK samples have a mass between 10–15 mg and 19–25 mg respectively. Through this analysis, the effect of thermal degradation on the T_m, T_c, T_g and the DOC of PEEK and CF-PEEK is examined. To calculate the DOC of the examined samples, the second heating curve is analysed and Eq. (1) is used.

$$DOC(\%) = \frac{\Delta H_m}{\Delta H_f}(1-f)x100 \quad (1)$$

In Eq. (1), ΔH_m is the enthalpy of fusion at the melting point as measured by the area under the endothermic melting peak of the second heating cycle. Moreover, ΔH_f is the enthalpy of fusion of the fully crystalline PEEK which is equal to 130 J/g [38]. Finally, f stands for the sample's fibre content by weight which in our case is 66% (0.66) for CF-PEEK and zero for the pure PEEK.

3. Results and discussion

3.1. Thermogravimetric analysis

The conducted TGA experiments of PEEK and CF-PEEK in a 50 ml/min airflow with the applied heating rates of 5, 20, 50 and 100 °C/min are presented in Fig. 1a and Fig. 1b respectively. Overall, the decomposition of both PEEK and CF-PEEK in an air atmosphere is a two-step process and chain scission and crosslinking are the suggested mechanisms that occur upon the thermal degradation of PEEK and CF-PEEK [1,8,9,39].

The initial mechanism that takes place at the first step is the breakdown of the ketone and ether bonds of PEEK's monomer unit [7,40,41]. Then, during the second step the carbonaceous char that has been formed is oxidised resulting to the main products of the materials' decomposition which are CO, CO_2 phenols and aromatic ethers [39]. Comparing the decomposition behaviour of the two materials (Fig. 1), it is evident that the the CF enhances the thermal stability of PEEK [3]. For instance, for the samples heated with 5 °C/min the temperature where the 5% of the mass is lost ($T_{95\%}$) is equal to 549 °C in PEEK (Fig. 1a) and 555 °C in CF-PEEK (Fig. 1b). This difference is more significant for the samples heated with 100 °C/min where $T_{95\%}$ is equal to 597 °C in PEEK (Fig. 1a) and 615 °C in CF-PEEK (Fig. 1b). The above observations outline that the reinforced material is more thermally stable and they also show that the decomposition of PEEK and CF-PEEK in air offsets at higher temperatures at increased heating rates [39,42].

Another interesting observation can be made about the mass content that is decomposed during the first decomposition step. A mass content between 30% and 42% is lost during the first decomposition step in pure PEEK at the examined heating rates. Interestingly, an important mass loss is found to take place in a small temperature window (detail of Fig. 1a). Indicatively, the PEEK sample that has been heated with 5 °C/min loses 25% of its mass between 549 °C and 580 °C. On the other hand, the reinforced material loses approximately 10%-13% of its initial mass during the first decomposition step (detail of Fig. 1b). Nevertheless, the latter percentage refers mostly to the PEEK matrix content that predominantly decomposes during the first decomposition step of CF-PEEK.

To demonstrate the above, pure CF bundles of an initial mass around 8.1 mg are examined with TGA in a 50 ml/min airflow and in static air conditions with a heating rate of 5 °C/min (Fig. 2). As a matter of fact, the detail of Fig. 2 shows that in a 50 ml/min airflow the fibres start oxidising around 450 °C and have lost less than 2% of their mass up to 565 °C where the first decomposition step of CF-PEEK terminates when heated with 5 °C/min (detail of Fig. 1b). This observation outlines that it is the PEEK matrix content that is mostly affected during CF-PEEK's first decomposition step while the reinforcement remains relatively intact. Therefore, considering that the examined CF-PEEK samples have an initial PEEK mass content of 34% and 10%-13% of their initial mass is decomposed during the first decomposition step it is evident that a similar amount of PEEK content is actually decomposed at the pure and the reinforced material. Overall, the analysis shows that around 1/3 of PEEK's and CF-PEEK's initial PEEK mass content is lost during their first decomposition step in the examined air environment. In addtion, it is interesting to notice that the CF bundles examined in static air conditions also lost 1.2% of their initial mass up to 450 °C and an additional 1% up to 1000 °C (Fig. 2). The above demonstrates that the CF remains relatively intact in static air conditions as well. Finally, the 1.2% mass loss that occurs up to 450 °C in both the examined heating conditions (Fig. 2) is attributed to the decomposition of the organic-based sizing compound that takes place at the CFs under these conditions [43,44].

To conclude the TGA investigation, the effect of the heating rate on

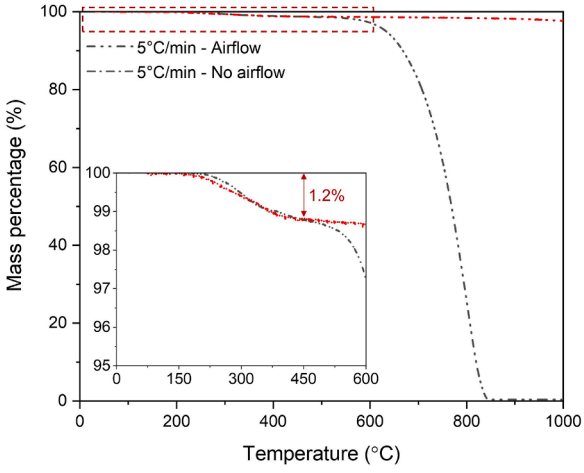

Fig. 2. TGA results of pure CFs in a 50 ml/min airflow and in static air conditions with a heating rate of 5 °C/min and detail of the results up to a 95% remaining mass (temperature window: 0–600°C).

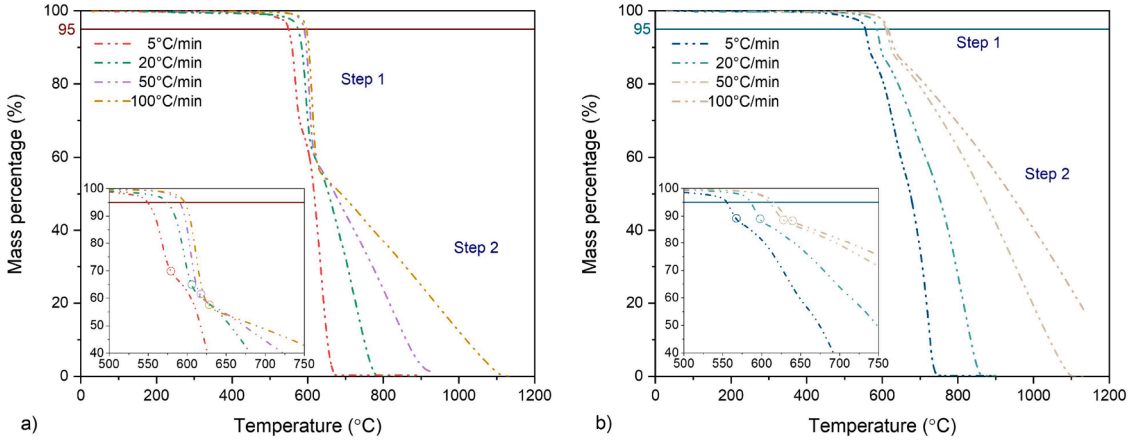

Fig. 1. Conducted TGA experiments of a) PEEK and b) CF-PEEK in a 50 ml/min airflow with heating rates of 5, 20, 50 and 100 °C/min.

the second decomposition step of PEEK and CF-PEEK is outlined. First of all, Fig. 1a shows that PEEK's decomposition terminates around 675 °C at a heating rate of 5 °C/min, while at 100 °C/min the decomposition is complete at temperatures above 1100 °C. Similarly, in CF-PEEK full decomposition occurs around 740 °C with a heating rate of 5 °C/min, while there is still a 18% of remaining mass at 1130 °C when a heating rate of 100 °C/min is applied (Fig. 1b). The above also outlines that the CF improves the thermal stability of the polymeric material. In addition, it is evident that faster heating rates offset the end of the second decomposition step at higher temperatures for both PEEK and CF-PEEK. As previously discussed, the oxidation of the carbonaceous char that has been previously formed takes place during the second decomposition step [39]. Therefore, considering that at higher heating rates there is lesser available time for the oxygen to diffuse into the material the oxidation mechanisms of the second decomposition step take place in a wider temperature window as the heating rate increases. The above explains why the temperature range where full decomposition occurs increases for both PEEK and CF-PEEK in faster heating rates.

In summary, the TGA investigation highlights the main degradation mechanisms that occur in pure and CF reinforced PEEK in an air atmosphere and illustrates their response in slower and faster heating rates. In both the examined materials, a two-step decomposition process occurs and chain scission and crosslinking mechanisms mainly take place during the first decomposition step, while in the second decomposition step the formed carbonaceous char is oxidised. Moreover, the analysis shows that the reinforced material is more thermally stable than the pure PEEK. Finally, the onset of thermal degradation that results in mass loss occurs at temperatures around 500 °C (Fig. 1). Nevertheless, it should be noted that the thermal degradation mechanisms initiate at lower temperatures where the materials' self-nucleation is not yet suppressed [45,46]. Several studies have used rheology characterisation techniques to examine the thermal degradation of PEEK before the event of mass loss [12,16,45]. They have also identified that upon PEEK's thermal degradation chain scission initially occurs followed by rapid branching reactions that ultimately lead to crosslinking [45].

3.2. ATR-FTIR

To establish a thermal degradation assessment methodology in rapid high-temperature processing of PEEK and CF-PEEK, samples that went through several heating programs in static air conditions with heating rates of 5, 20, 50 and 100 °C/min are examined with ATR-FTIR. Specifically, partially degraded PEEK samples that have lost 0.5%, 1.2%, 4% and 15% of their initial mass and partially degraded CF-PEEK samples that have lost 0.25%, 0.6%, 1.7% and 6.7% of their initial mass are examined. Through this process, the spectral changes that occur in PEEK and CF-PEEK with the progress of thermal degradation are detected. In addition, a methodology is proposed for assessing the extent of thermal degradation that occurs in PEEK and CF-PEEK in applications where rapid high-temperature processing is applied. Initially, before presenting the results of this investigation, the infrared spectrum of the as-received pure PEEK is presented and discussed.

3.2.1. The infrared spectrum of as-received PEEK

The spectrum of PEEK has been examined and discussed by several researchers in the public domain literature [47–49]. It is the chemical repeat unit of PEEK that leads to its enhanced thermal stability [39] (Fig. 3). Additionally, the characteristic spectrum of pure PEEK is also presented in the spectral region between 1800-600 cm^{-1} (Fig. 4). Similar spectra are identified at PEEK and CF-PEEK and overall the peaks in their spectra are assigned according to the various groups of PEEK's chemical repeat unit (Fig. 3).

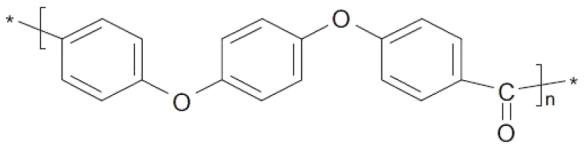

Fig. 3. The chemical repeat unit of PEEK.

In the infrared spectrum of PEEK and CF-PEEK the carbonyl region is found between 1800 and 1600 cm^{-1}, the ether and the ester region is found between 1350 and 1100 cm^{-1} and the aromatic hydrogens are found below 900 cm^{-1} [1]. The significant spectral features are the carbonyl peak at 1653 cm^{-1}, the phenyl ring stretching bands at 1593 cm^{-1}, 1486 cm^{-1} and 1410 cm^{-1} and the bending motion of the group (C–C(=O)–C) at 1305 cm^{-1}. Moreover, at 1277 cm^{-1}, 1216 cm^{-1} and 1185 cm^{-1} the asymmetric stretching of the diphenyl ether group is identified. Finally, between 1200-600 cm^{-1} phenyl ring C-H deformations are mainly found in the spectra of PEEK [30,50].

3.2.2. The effect of thermal degradation on PEEK's and CF-PEEK's infrared spectrum

To identify the spectral changes that occur upon thermal degradation, PEEK and CF-PEEK samples that have surpassed the melting stage without having reached though the onset of degradation are examined as well as samples that have experienced a maximum mass loss of 15% and 6.7% respectively. Furthermore, to examine the response of the materials in slower and faster heating the examined PEEK and CF-PEEK samples were partially degraded with a heating rate of 5, 20, 50 and 100 °C/min. The examined PEEK and CF-PEEK samples showed the same response and similar spectral changes were identified with the progress of thermal degradation in the examined heating rates. These changes are mainly a result of the chain scission and the crosslinking mechanisms that take place upon the thermal degradation of PEEK and CF-PEEK in an air environment [8,39,51]. First of all, between 4000 and 1800 cm^{-1}, limited spectral changes are noticed and mainly an increase in the intensity of the non-aromatic hydrogen carbon bonds at 3064, 2923 and 2851 cm^{-1} is identified. Those changes are attributed to the degradation of the fragmented phenyl rings that result from the chain scission that occurs in the monomer of PEEK with the applied heating [15].

On the other hand, significant spectral changes are found in the frequency ranges between 1800 and 600 cm^{-1} (Fig. 5). In Fig. 5, the first two arrows indicate the existence of two new peaks at 1711 cm^{-1} and at 1452 cm^{-1}. Moreover, the growth of a shoulder is detected in the high frequency side of the ether peak at 1216 cm^{-1} as well as changes at the diphenylether bonds around 1110 cm^{-1}. Finally, changes at the intensity ratio between the 966 cm^{-1} and the 952 cm^{-1} are noticed with degradation as well as changes at the aromatic rings around 850 cm^{-1} (Table 1). To provide a greater amount of information, the spectral regions between 1800-1350 cm^{-1} and between 1350 and 600 cm^{-1} are

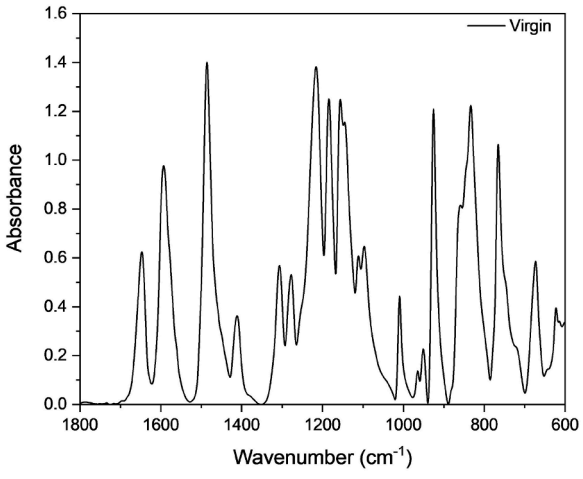

Fig. 4. FTIR spectra of pure PEEK between 1800-600 cm^{-1} (baseline-corrected and normalised to 1593 cm^{-1}).

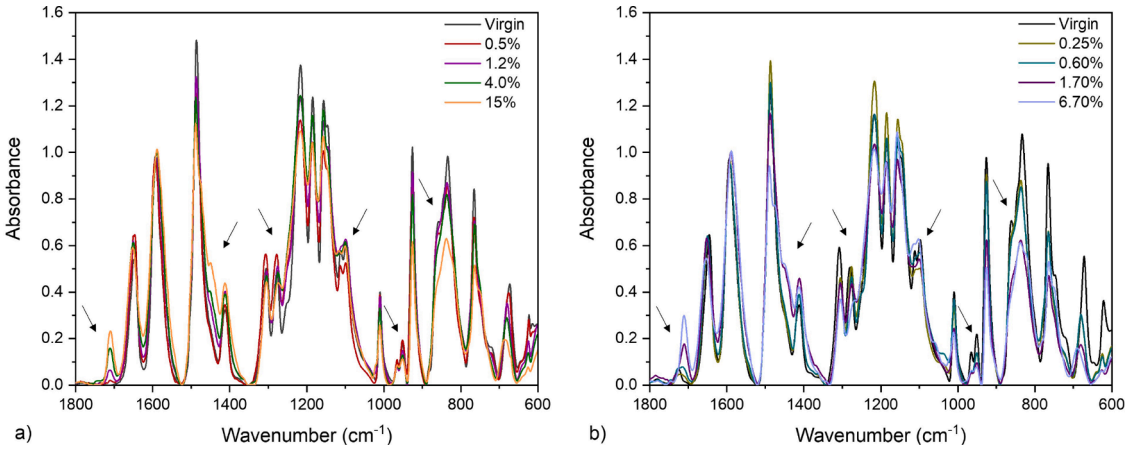

Fig. 5. Spectral changes that occur at a) PEEK and b) CF-PEEK upon thermal degradation when heated with 50 °C/min up to a 0.5%, 1.2%, 4%, 15% and a 0.25%, 0.6%, 1.7%, 6.7% mass loss respectively (1800-600 cm^{-1}).

Table 1
Main spectral changes identified in PEEK and CF-PEEK upon thermal degradation at 1800-600 cm^{-1}.

Wavenumber (cm^{-1})	Spectral changes upon thermal degradation (1800-600 cm^{-1})
1711, 1452	Formation of a new fluorenone peak
1253	Growth of a shoulder in the high-frequency side of the ether peak at 1216 cm^{-1}
1100	Changes in the diphenylether bonds
966, 952	Changes in the intensity ratio of the two bands
863, 841	Changes in the aromatic rings

presented in detail in Figs. 6 and 7 respectively.

In both the examined materials, the most evident change is the development of a new peak in the carbonyl region and particularly at 1711 cm^{-1} (Fig. 6). This new peak whose intensity gets stronger as degradation progresses is also found in recent studies that examined the thermal aging of PEEK [7] and its response to ion irradiation [30]. It is attributed to the formation of a fluorenone-type structure as a degradation product. It was firstly mentioned in the studies of Cole et al., where PEEK and CF-PEEK samples were exposed to isothermal heating in the range of 400–485 °C for a maximum duration of 480 min [50,52]. Furthermore, the second new peak at 1452 cm^{-1} also enhances its identification as a fluorenone-type structure especially after considering that the simple compound 9-fluorenone has its carbonyl absorption at 1715 cm^{-1} and a strong peak near 1450 cm^{-1} [50]. Finally, the fluorenone's formation mechanism is presented in Fig. 8 which illustrates the cyclization of the diradical that takes place in PEEK and CF-PEEK upon the event of thermal degradation [50].

It should also be mentioned that in studies where PEEK's response is examined at lower temperatures and long-time heating, another peak is also detected at 1739 cm^{-1}. This peak has been attributed to the formation of phenyl benzoate, which overall requires the presence of oxygen to form [7]. In our study though, where rapid high-temperature processing is applied there is not sufficient time for the diffusion of oxygen that would result in the formation of phenyl benzoate. Therefore, fluorenone is the major product in the carbonyl region of PEEK and CF-PEEK (Fig. 6). The above observation also agrees with the results of Cole et al. that identified the predominance of phenyl benzoate over fluorenone at lower temperatures ($\leq$ 400 °C) and longer heating and the inverse behaviour when higher temperatures were applied for a shorter duration [50].

In Fig. 7, the spectral changes that occur upon the thermal degradation of PEEK and CF-PEEK are displayed in the spectral region between 1350-600 cm^{-1}. First of all, in the examined spectral region the ester and ether region is found (1350-1100 cm^{-1}) where the main bands are the bending motion of the group (C–C(=O)–C) at 1305 cm^{-1} and the asymmetric stretching of the diphenyl ether group at 1277 cm^{-1}, 1216 cm^{-1} and 1185 cm^{-1}. In addition, in the spectral region between 1100-600 cm^{-1} phenyl ring C–H deformations are mainly identified. The major bands of this region are the C–H in-plane deformation band at 1010 cm^{-1}, the diphenyl ketone band at 925 cm^{-1}, two overlapping broad

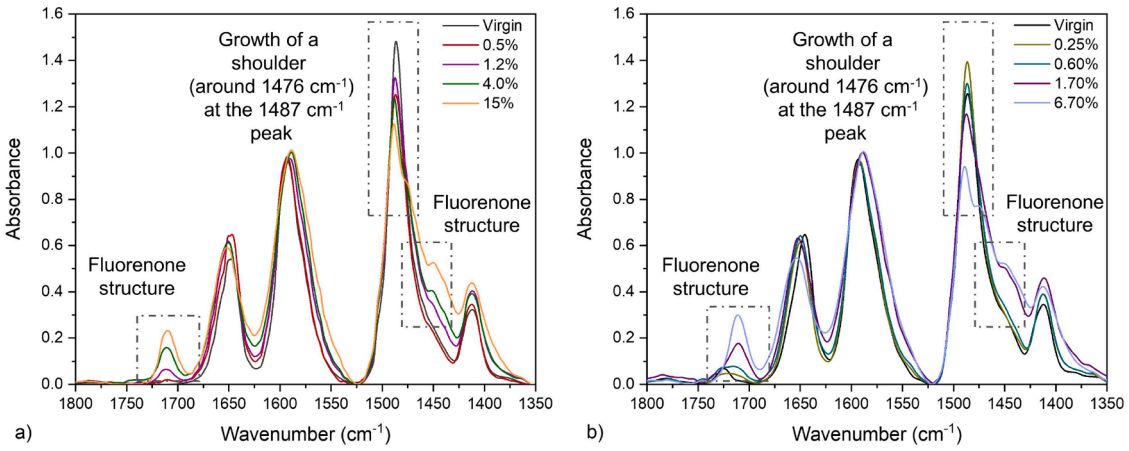

Fig. 6. Spectral changes that occur at a) PEEK and b) CF-PEEK upon thermal degradation when heated with 50 °C/min up to a 0.5%, 1.2%, 4%, 15% and a 0.25%, 0.6%, 1.7%, 6.7% mass loss respectively (1800-1350 cm^{-1}).

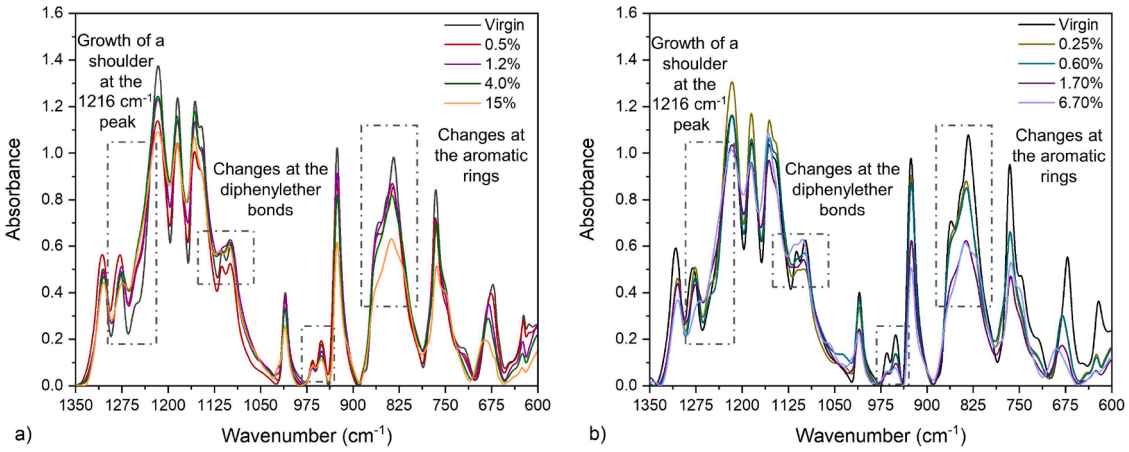

Fig. 7. Spectral changes that occur at a) PEEK and b) CF-PEEK upon thermal degradation when heated with 50 °C/min up to a 0.5%, 1.2%, 4%, 15% and a 0.25%, 0.6%, 1.7%, 6.7% mass loss respectively (1350-600 cm^{-1}).

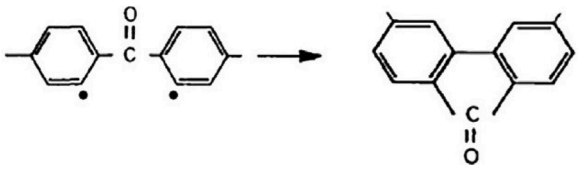

Fig. 8. The formation mechanism of fluorenone - Cyclization of the diradical.

bands at 863 and 841 cm^{-1} (aromatic hydrogens) and a band at 765 cm^{-1} [30].

The effect of thermal degradation does not lead to the formation of any new peaks in that region. Nonetheless, significant spectral changes are identified which have been attributed to the crosslinking mechanisms that take place at PEEK's aromatic ring with the applied high-temperature processing [1,30]. As shown in Fig. 7, in the ester and ether region a growth of a shoulder in the 1253 cm^{-1} peak takes place around 1216 cm^{-1} and changes in the diphenylether bonds around 1100 cm^{-1} are observed. Finally, between 1100-600 cm^{-1} changes in the overlapping broad bands of the aromatic hydrogens at 863 cm^{-1} and 841 cm^{-1} are noticed as well as changes in the intensity ratio of the 963 cm^{-1} and 952 cm^{-1} bands (Fig. 7). Interestingly, Chalmers et al. have found that the 963/952 cm^{-1} intensity ratio is a linear function of PEEK's crystallinity [46,49]. In our case study, changes of this intensity ratio were more evident in CF-PEEK, but in both the materials the 963/952 cm^{-1} intensity ratio was found to decrease with the progress of thermal degradation. Considering that the materials become more amorphous upon thermal degradation and their crystallinity content reduces, these findings agree with the observations of Chalmers et al. Nevertheless, to examine the effect of thermal degradation on the crystallinity of PEEK and CF-PEEK a DSC analysis takes place in the second part of this study.

In summary, the described spectral changes that are highlighted in PEEK and CF-PEEK in the spectral region between 1800-600 cm^{-1} are identified in all of the examined heating rates with the progress of degradation. °One of the significant spectral changes is the formation of the new fluorenone peak in 1711 cm^{-1}. This peak could be of considerable significance for the research community especially after considering that its intensity is found to increase with the progress of thermal degradation. To provide a thorough investigation on the above, a correlation between the extent of degradation that occurs in PEEK and CF-PEEK and the 1711 cm^{-1} peak's intensity takes place below.

3.2.3. A correlation between the 1711 cm^{-1} peak's intensity and the resulting extent of thermal degradation

The fluorenone peak that develops in the carbonyl region has also been observed in studies that examined PEEK and CF-PEEK subject to long-time heating [7,50,52]. Its formation around 1711 cm^{-1} is attributed to a fluorenone-type structure and, overall, its development has been associated with the process of degradation [14]. Nevertheless, its applicability as a tool for characterising the extent of thermal degradation that occurs in PEEK and CF-PEEK after rapid high-temperature processing has not been examined yet. Therefore, in this study the development of the fluorenone peak at faster and slower heating rates is examined and its applicability as a degradation characterisation tool is assessed. It has already been shown that its intensity increases with thermal degradation at the PEEK and CF-PEEK samples that are partially degraded with a heating rate of 50 °C/min (Fig. 6). To demonstrate the described association in all of the examined heating rates, fluorenone's development at the examined PEEK and CF-PEEK samples that have been heated upon thermal degradation with 5, 20 and 100 °C/min is also presented in Fig. 9 and Fig. 10 respectively. Through this process, the applicability of the 1711 cm^{-1} peak's intensity as a thermal degradation detection and characterisation tool in rapid high-temperature processing of PEEK and CF-PEEK is demonstrated. Moreover, its advantageous use in studies that aim to optimise rapid high-temperature applications of PEEK and CF-PEEK is highlighted.

To begin with, the spectra presented in Figs. 9 and 10 have also been baseline-corrected and normalised to the 1593 cm^{-1} peak. The results show that a similar behaviour takes place at the examined heating rates and the intensity of the 1711 cm^{-1} peak increases with thermal degradation in both PEEK and CF-PEEK. Interestingly, the peak starts to develop when 0.5% of PEEK's initial mass is lost and it is profound when the mass loss surpasses 1% (Fig. 9). Similarly, its formation has initiated in the CF-PEEK samples that have lost 0.25% of their initial mass and is clearly evident when the samples have degraded by 0.6% (Fig. 10). Taken together, the analysis shows that in both the materials its development is directly linked with the onset of thermal degradation in all the examined heating rates. Therefore, it could consist a valid detection criterion for identifying which processing conditions slightly trigger the degradation mechanisms of PEEK and CF-PEEK in rapid high-temperature processing.

In addition, the significant increase that is identified in the peak's intensity as degradation progresses, clearly demonstrates its association with thermal degradation. To outline the above, the average value and standard deviation of fluorenone's intensity is presented for the PEEK and CF-PEEK samples that are heated with the examined heating rates upon the examined mass loss percentages (Fig. 11). As previously mentioned, three samples are examined for each heating program and five different measurements take place for each sample and the accumulated spectra are baseline-corrected and normalised to the 1593 cm^{-1}

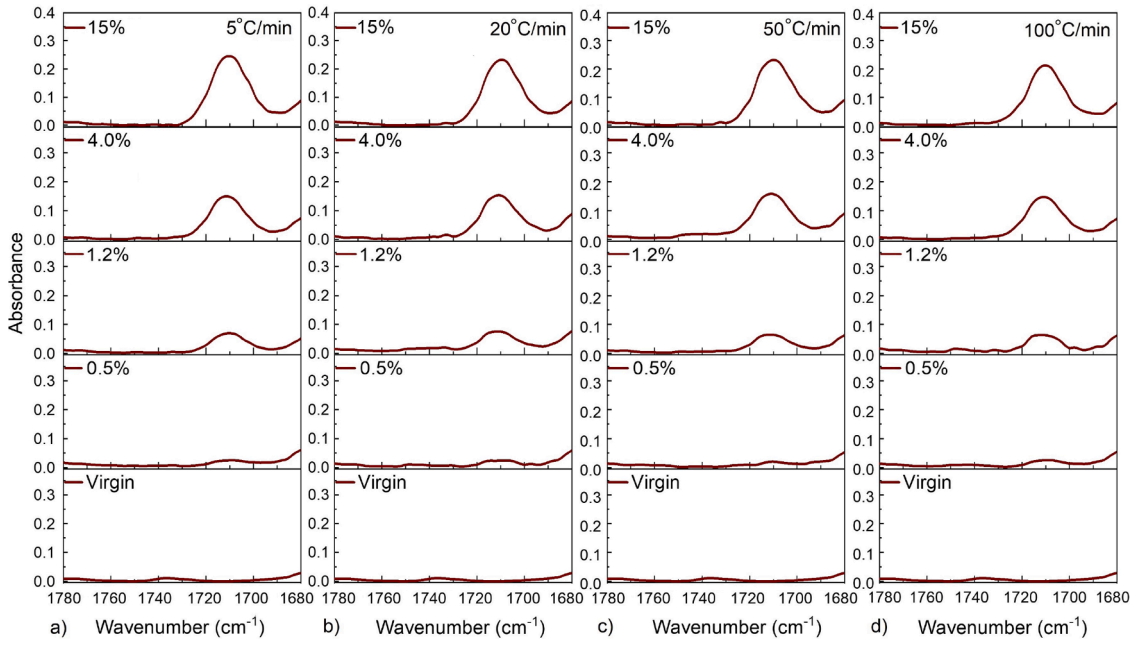

Fig. 9. The development of the 1711 cm^{-1} peak in PEEK samples heated in static air conditions with 5, 20, 50 and 100 °C/min up to a resulting mass loss of 0.5%, 1.2%, 4% and 15%.

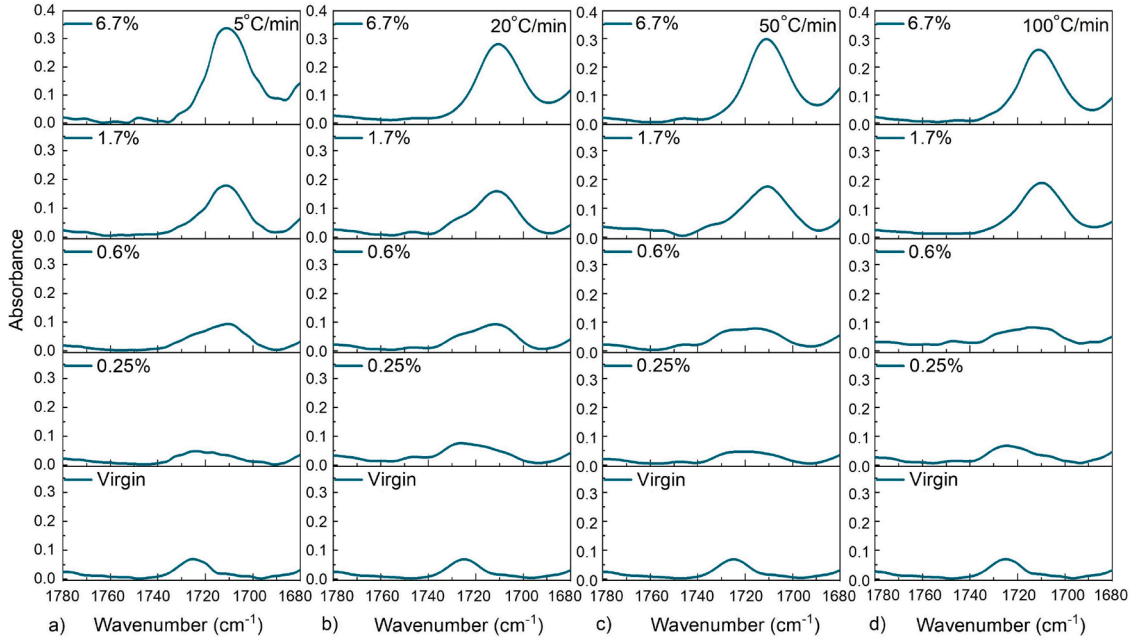

Fig. 10. The development of the 1711 cm^{-1} peak in CF-PEEK samples heated in static air conditions with 5, 20, 50 and 100 °C/min up to a resulting mass loss of 0.25%, 0.6%, 1.7% and 6.7%.

peak.

In Fig. 11a, the 1711 cm^{-1} peak's average intensity across the examined heating rates is 0.019, 0.042, 0.12 and 0.217 for a mass loss of 0.5%, 1.2%, 4% and 15% respectively. Despite the significantly different dwell time that the samples experience at temperatures above PEEK's melting point, the resulting intensity is found similar across the examined heating rates at each one of the examined mass loss percentages. Interestingly, clear regions are found and no overlapping is noticed between the applied heating rates even at levels of degradation that are in close proximity with each other (e.g. 0.5% and 1.2%). The above findings demonstrate that the peak's intensity could be used for identifying the approximate extent of the resulting thermal degradation in PEEK after an applied heating process with heating rates up to 100 °C/min.

Likewise, in Fig. 11b no overlapping is noticed in CF-PEEK across the different mass loss percentages at the examined heating rates. In CF-PEEK, the average intensity of the 1711 cm^{-1} peak is around 0.039, 0.085, 0.167 and 0.275 for a mass loss of 0.25%, 0.6%, 1.7% and 6.7% respectively. The fact that fluorenone's development in CF-PEEK takes place in a similar manner in slower and faster heating, also demonstrates its applicability as a tool for detecting and characterising the extent of CF-PEEK's thermal degradation when it is processed with rapid high-

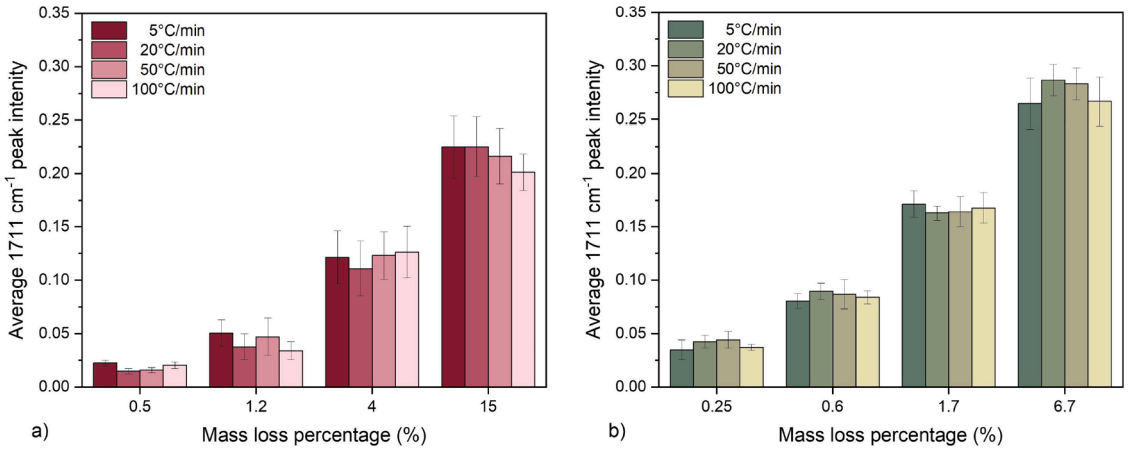

Fig. 11. Average intensity and standard deviation of the 1711 cm^{-1} peak, when PEEK and CF-PEEK are heated with 5, 20, 50 and 100 °C/min upon a mass loss of: a) 0.5%, 1.2%, 4%, 15% and b) 0.25%, 0.6%, 1.7%, 6.7% respectively.

temperature processing.

The above analysis highlights the correlation that exists between the 1711 cm^{-1} peak's intensity and the thermal degradation that takes place in PEEK and CF-PEEK in static air conditions. A similar behaviour is identified in both the materials and in all the examined heating rates. This demonstrates the capability of using the 1711 cm^{-1} peak's intensity for detecting and characterising the extent of thermal damage that can take place in applications of PEEK and CF-PEEK where fast heating is applied. The above could consist a significant tool for the research community and the industry especially for optimising high-temperature applications of PEEK and CF-PEEK where rapid high-temperature processing is applied. For instance, it could be used for detecting the processing conditions that would not induce a significant thermal damage in PEEK and CF-PEEK, further defining therefore the materials' optimum process window in these applications. Taken together, to facilitate the use of the 1711 cm^{-1} peak's intensity as a detection and characterisation tool, its intensity values in the heating programs of this study are gathered in Table 2.

3.2.4. Activation energy of the 1711 cm^{-1} peak's formation mechanism in PEEK and CF-PEEK

To further examine the 1711 cm^{-1} peak's formation mechanism in the applied static air conditions, its activation energy in both PEEK and CF-PEEK is calculated. Through this process, the effect of the reinforcement on the fluorenone's formation rate is examined. To begin with, to calculate the activation energy of the 1711 cm^{-1} peak's formation mechanism several PEEK samples are isothermally heated at 430, 460 and 490 °C for exposure times that vary between 10 and 120 min (Fig. 12). In Fig. 12a, the 1711 cm^{-1} peak's intensity normalised to the 1593 cm^{-1} peak is shown as a function of the exposure time when heated at 430, 460 and 490 °C. In Fig. 12a, the slope of each line represents the fluorenone's growth rate in each temperature and in Fig. 12b the Arrhenius plot of fluorenone's growth rate is presented. The activation energy of fluorenone is found to be 218.1 kJ/mol in pure PEEK when it is heated in static air conditions. The above value is close to the value found by Cole et al. that also examined PEEK samples in air with similar heating conditions [50].

To calculate the activation energy of the fluorenone's formation mechanism in CF-PEEK, a process similar to the one for PEEK takes place. In particular, several CF-PEEK samples are heated at 430, 460 and 490 °C for exposure times that vary between 10 and 120 min. In Fig. 13a, the 1711 cm^{-1} peak's intensity normalised to the 1593 cm^{-1} peak is shown as a function of the exposure time for the three examined temperatures and in Fig. 13b the Arrhenius plot of the fluorenone's growth rate is presented. Through this process, the activation energy of the 1711 cm^{-1} peak's formation mechanism is found to be 207.7 kJ/mol in CF-PEEK, which is also similar to the value defined by Cole et al. for APC-2 laminates heated in an air atmosphere [52]. Taken together, a slightly lower activation energy is found in CF-PEEK and overall the analysis captures a similar fluorenone's growth rate in the pure and the reinforced material.

3.2.5. A comparison between the 1711 cm^{-1} peak's intensity in thermally degraded PEEK and CF-PEEK

In Fig. 11, it is shown that the 1711 cm^{-1} peak's intensity in CF-PEEK was greater in significantly lower mass loss percentages than in pure PEEK. Indicatively, the average intensity of the 1711 cm^{-1} peak is around 0.275 in the CF-PEEK samples with a 6.7% mass loss. On the other hand,

Table 2
The 1711 m^{-1} peak's intensity in PEEK and CF-PEEK after being heated with 5, 20, 50, 100 °C/min up to the examined mass loss percentages and average intensity per mass loss percentage across the examined heating rates.

Mass loss	PEEK Heating rate				Average intensity
	5 °C/min	20 °C/min	50 °C/min	100 °C/min	
0.5%	0.023± 0.0025	0.015± 0.0025	0.016±0.0023	0.020± 0.0029	0.019±0.0037
1.2%	0.050± 0.0125	0.038± 0.0119	0.047±0.0175	0.034± 0.0085	0.042±0.0077
4.0%	0.121± 0.0247	0.111± 0.0259	0.123± 0.0221	0.126± 0.0242	0.120±0.0067
15%	0.225± 0.0293	0.225± 0.0283	0.216± 0.0258	0.201± 0.0169	0.217±0.0112
Mass loss	CF-PEEK Heating rate				Average intensity
	5 °C/min	20 °C/min	50 °C/min	100 °C/min	
0.25%	0.035± 0.0092	0.043± 0.0060	0.044± 0.0078	0.037± 0.0027	0.040±0.004
0.6%	0.081±0.0069	0.090±0.0075	0.087±0.0139	0.084±0.0062	0.085±0.004
1.7%	0.171±0.0124	0.163±0.0069	0.164±0.0142	0.168±0.0145	0.167±0.004
6.7%	0.265±0.0236	0.286±0.0145	0.283±0.0149	0.267±0.0225	0.275± 0.011

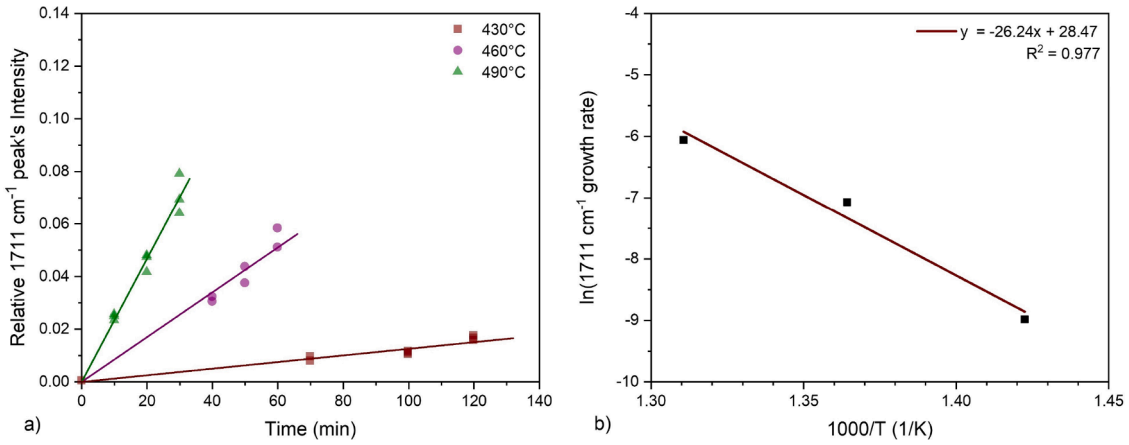

Fig. 12. a) Growth of the 1711 cm^{-1} peak in PEEK as a function of the exposure time at 430, 460 and 490 °C and b) Arrhenius plot of the 1711 cm^{-1} peak's growth rate when PEEK is heated in static air conditions.

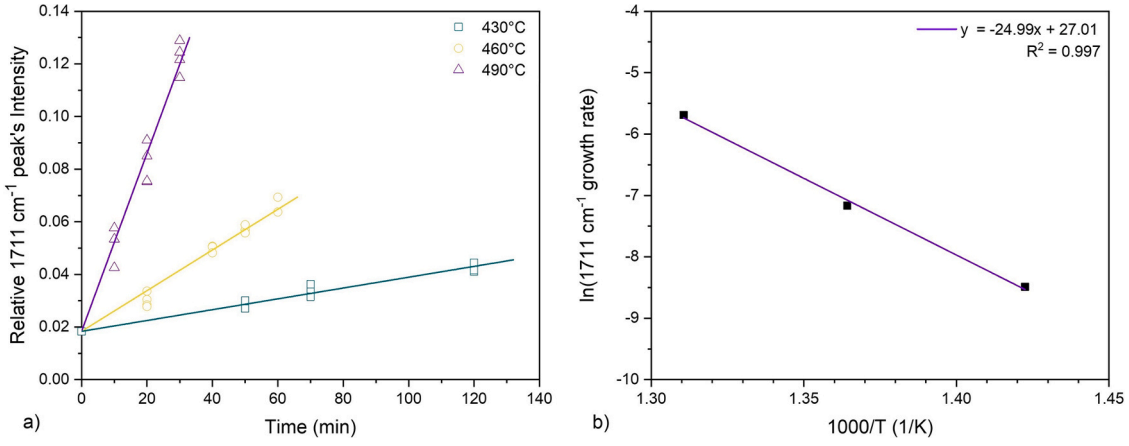

Fig. 13. a) Growth of the 1711 cm^{-1} peak in CF-PEEK as a function of the exposure time at 430, 460 and 490 °C and b) Arrhenius plot of the 1711 cm^{-1} peak's growth rate when CF-PEEK is heated in static air conditions.

in the PEEK samples with a 15% mass loss the average 1711 cm^{-1} peak's intensity is around 0.217 across the four examined heating rates (Table 2). To explain the observed difference, it should be highlighted once again that at the examined temperatures it is the PEEK matrix content of the reinforced material that is mostly affected in static air conditions while the CFs remain relatively intact (Fig. 2). As shown in Fig. 2, the mass loss that occurs in the CF in static air conditions is mostly due to the degradation of its organic-based sizing compound [43,44]. Hence, the resulting mass loss in the examined CF-PEEK samples mostly refers to the amount of their decomposed PEEK matrix content. For instance, in the samples that lost 6.7% of their initial mass less than 1% would be due to the decomposed sizing agent and around 6% would be due to the decomposed PEEK matrix content. The latter is approximately the 17.5% of the overall PEEK content of the examined CF-PEEK samples. Therefore, this explains why higher values of the 1711 cm^{-1} peak's intensity are captured in significantly lower levels of CF-PEEK's degradation.

Considering the above, to accurately use the 1711 cm^{-1} peak's intensity for characterising the extent of CF-PEEK's thermal degradation, the V_f of the examined CF-PEEK sample should be considered. To make things clearer, the same heating conditions would result in a different extent of degradation in CF-PEEK samples with different fibre volume fractions. Therefore, it would be recommended to use the 1711 cm^{-1} peak's intensity that is found in pure PEEK as a tool for characterising the extent of thermal degradation in CF-PEEK, by taking also into account the sample's V_f and the decomposition of the CF's sizing agent. This approach would reduce the implications that exist when reinforced samples with different fibre contents and sizing agents are examined. It would therefore further establish the intensity of the fluorenone peak as a universal tool for assessing the thermal degradation of both PEEK and CF-PEEK when rapid high-temperature processing is applied.

3.3. *Differential scanning calorimetry*

It is long recognised that the mechanical properties of semi-crystalline polymers like PEEK are highly dependent on the polymer's DOC [31–35]. In general, a higher crystallinity content of the polymeric material leads to improved mechanical properties [33,36,37]. An important parameter that affects the crystallinity content of PEEK and CF-PEEK in high-temperature processing is the applied cooling rate. It is the slower cooling that favours the formation of crystalline morphology at semi-crystalline polymers like PEEK [33]. At fast manufacturing technologies though, like LATP applications [35], pultrusion [53] or induction heating [18] high temperatures are applied for a short amount of time and the processed materials are then commonly let to naturally cool down to room temperature [54]. Therefore, natural cooling takes place in the examined PEEK and CF-PEEK samples of this study and to further assess the effect of rapid high-temperature processing on PEEK and CF-PEEK the partially degraded samples are examined with DSC. Through this investigation, the extent of thermal degradation that does not severely affect the crystallinity content of PEEK and CF-PEEK and consequently would not severely deteriorate their mechanical properties

is examined. In addition, the effect of the applied heating rate is also assessed and PEEK's and CF-PEEK's overall response at slower and faster heating is investigated.

In Fig. 14, it is shown that the endothermic melting peak (T_m) and the exothermic crystallisation peak (T_c) of PEEK shift to lower temperatures as degradation progresses. Moreover, the overall melting and crystallization process takes place in a wider temperature window with the progress of thermal degradation. The above are particularly evident in the PEEK samples that have lost 0.5%, 1.2% and 4% of their initial mass. In the samples that have lost 15% of their mass no melting and crystallisation peaks are identified. This demonstrates that PEEK has become completely amorphous in that mass loss percentage. In addition, the area under the endothermic and the exothermic peaks reduces upon thermal degradation which shows that the material's crystallinity content also reduces. This tendency is captured in all of the examined heating rates and a similar behaviour is identified in CF-PEEK as well. In Fig. 15, the T_m and T_c of CF-PEEK also shift to lower temperatures with the progress of thermal degradation and the area under the two peaks reduces as well. The latter demonstrates that the amorphous content of the material increases with the progress of thermal degradation. As a matter of fact, in all the examined heating rates a mass loss of 1.7% and 6.7% resulted in completely amorphous CF-PEEK samples and no melting and crystallisation peaks were found in these samples (Fig. 15).

3.3.1. *The effect of thermal degradation on the T_m, T_c and T_g of PEEK and CF-PEEK*

The progress of thermal degradation had the same effect on the T_m, T_c and T_g of PEEK and CF-PEEK in all of the examined heating rates. The T_m and T_c of PEEK (Fig. 16) and of CF-PEEK (Fig. 17) shift to lower temperatures with the progress of thermal degradation. On the other hand, the T_g of the examined PEEK and CF-PEEK samples increases as the thermal degradation progresses (Fig. 18). The observed shift of PEEK's and CF-PEEK's melting points to lower temperatures together with the increase in their glass transition temperature is a result of the crosslinking mechanisms that take place in PEEK and CF-PEEK upon the event of thermal degradation [1]. When crosslinking takes place, the polymer backbones are getting tied together and therefore the materials' molecular mobility reduces. Consequently, the resulting lack of molecular mobility decreases the amount of energy that is required for the melting to take place. Hence, the higher crosslinking density shifts PEEK's and CF-PEEK's T_m to lower temperatures and also shifts their transition to the rubbery state at higher temperatures as well (increase of T_g).

3.3.2. *The effect of thermal degradation on the crystallinity content of PEEK and CF-PEEK*

To conclude the DSC analysis, the effect of thermal degradation on PEEK's and CF-PEEK's crystallinity content is examined. As described in Section 2.2.3, to calculate the DOC of the examined samples the area under the endothermic melting peak of the second heating curve is calculated and is then used in Eq. (1). The results of the analysis are presented in Fig. 19 and the effect of thermal degradation on PEEK's and CF-PEEK's crystallinity content is illustrated when the materials are partially degraded with the four examined heating rates of this study.

In Fig. 19, it is shown that thermal degradation reduces the DOC of PEEK and CF-PEEK in all of the examined heating rates. As previously mentioned, the PEEK samples with a 15% mass loss and the CF-PEEK samples with a 1.7% and a 6.7% mass loss are completely amorphous and therefore they are not included in the results of Fig. 19. The observed reduction in the crystallinity content of PEEK and CF-PEEK was also indicated from the reduced area under PEEK's and CF-PEEK's endothermic melting peaks in Fig. 14a and Fig. 15a respectively. As mentioned above, the crosslinking mechanisms that take place upon the thermal degradation of PEEK and CF-PEEK reduce their molecular mobility. This deteriorates the capability of the materials to rearrange their molecules in a structural order during the cooling process. Therefore, a higher level of degradation results in a more amorphous PEEK and CF-PEEK with less desirable mechanical properties.

Interestingly though, the crystallinity content of the PEEK samples that experience a 0.5% and 1.2% mass loss remains in similar levels with the crystallinity content of the virgin material (Fig. 19a). A similar behaviour is also identified in the CF-PEEK samples that experience a 0.25% mass loss (Fig. 19b). Moreover, the above observations are more evident in the samples that are heated with faster heating rates. Hence, the analysis shows that the effect of thermal degradation on the DOC of PEEK and CF-PEEK reduces as the heating rate increases. For instance, the PEEK and CF-PEEK samples that are partially degraded with a heating rate equal to 5 °C/min are the ones with the greatest reduction in their crystallinity content. On the other hand, the samples that are heated with 50 and 100 °C/min show the highest DOC in all of the examined mass loss percentages.

From the above analysis two main conclusions can be made. First of all, it is shown that a level of degradation close to 1% for PEEK and around 0.25% for CF-PEEK does not severely impact their crystallinity content. Considering though that the 0.25% of CF-PEEK's decomposed mass mostly refers to its decomposed PEEK matrix content (Fig. 2), this percentage consists approximately the 0.85% of the reinforced sample's overall PEEK content. Therefore, both the investigations of Fig. 19 indicate that a degradation around 1% of the materials' PEEK content could be considered acceptable as far as their DOC is concerned. In

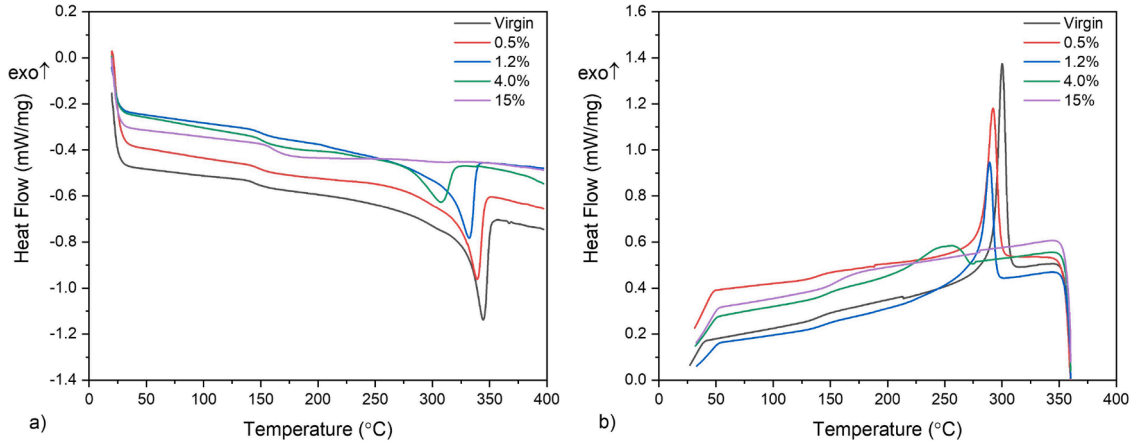

Fig. 14. DSC thermograms of a) the second heating cycle and b) the cooling cycle for the virgin PEEK and the PEEK samples that have lost 0.5%, 1.2%, 4% and 15% of their initial mass (heating rate: 100 °C/min).

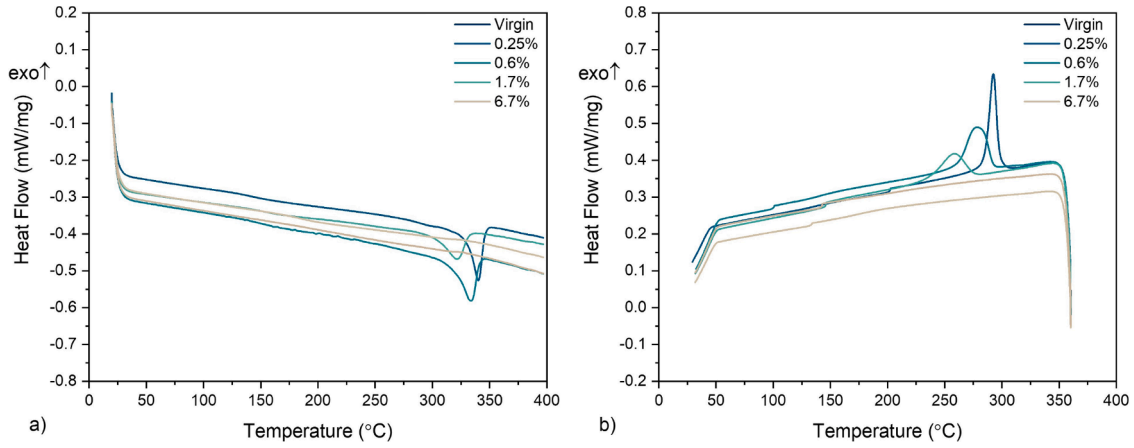

Fig. 15. DSC thermograms of a) the second heating cycle and b) the cooling cycle for the virgin CF-PEEK and the CF-PEEK samples that have lost 0.25%, 0.6%, 1.7% and 6.7% of their initial mass (heating rate: 50 °C/min).

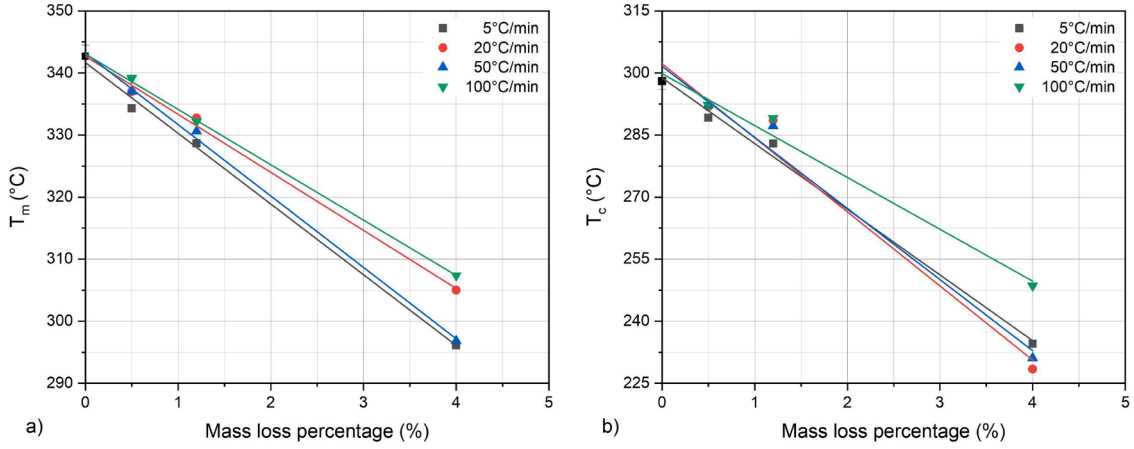

Fig. 16. a) T_m and b) T_c of PEEK as degradation progresses for the heating rates of 5, 20, 50 and 100 °C/min.

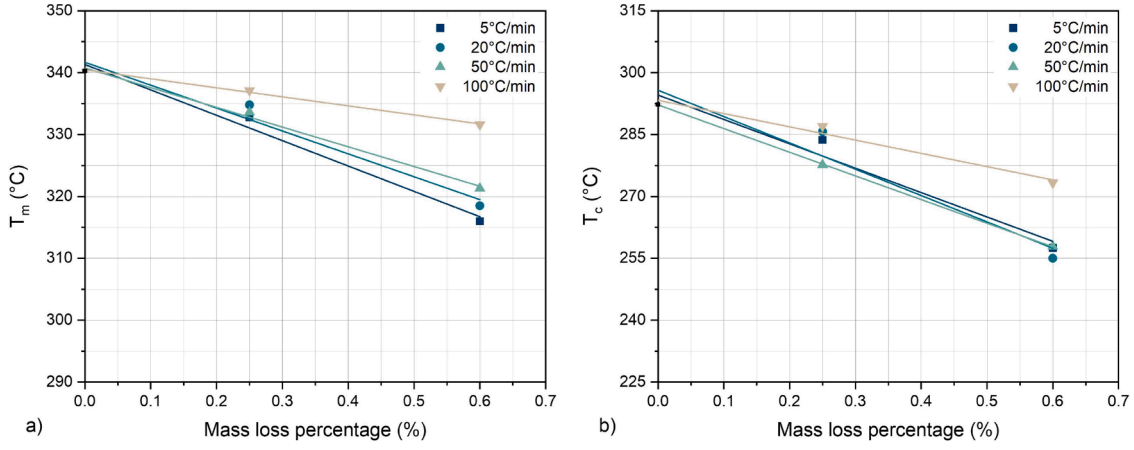

Fig. 17. a) T_m and b) T_c of CF-PEEK as degradation progresses for the heating rates of 5, 20, 50 and 100 °C/min.

addition, in both PEEK and CF-PEEK an increased heating rate has a reduced effect on their DOC. This has to do with the time-dependency of the crosslinking mechanisms that take place upon thermal degradation. For instance, by increasing the heating rate from 5 °C/min to 100 °C/min the dwell time that the PEEK and CF-PEEK samples remain above their melting temperatures reduces by 20 times. Therefore, the reduced amount of time that the materials remain at high temperatures when higher heating rates are applied has a smaller effect on their crystallinity content. This is the main reason that the faster heating rates affect the DOC of PEEK and CF-PEEK to a lesser extent when the materials are heated upon thermal degradation (Fig. 19). To conclude the analysis, the T_m, T_g, T_c and the DOC of the examined PEEK and CF-PEEK samples are presented in Table 3 and Table 4 respectively.

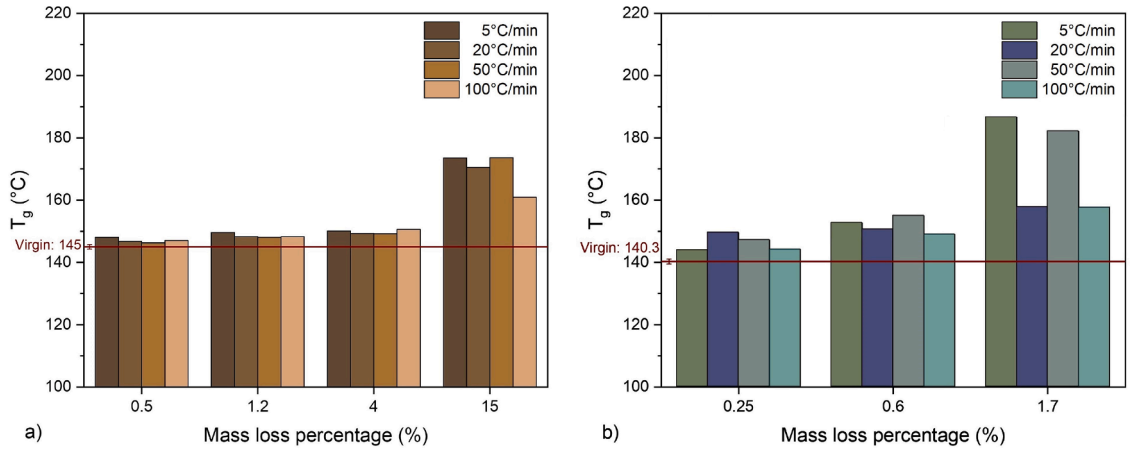

Fig. 18. T_g of a) PEEK and b) CF-PEEK as degradation progresses for the heating rates of 5, 20, 50 and 100 °C/min.

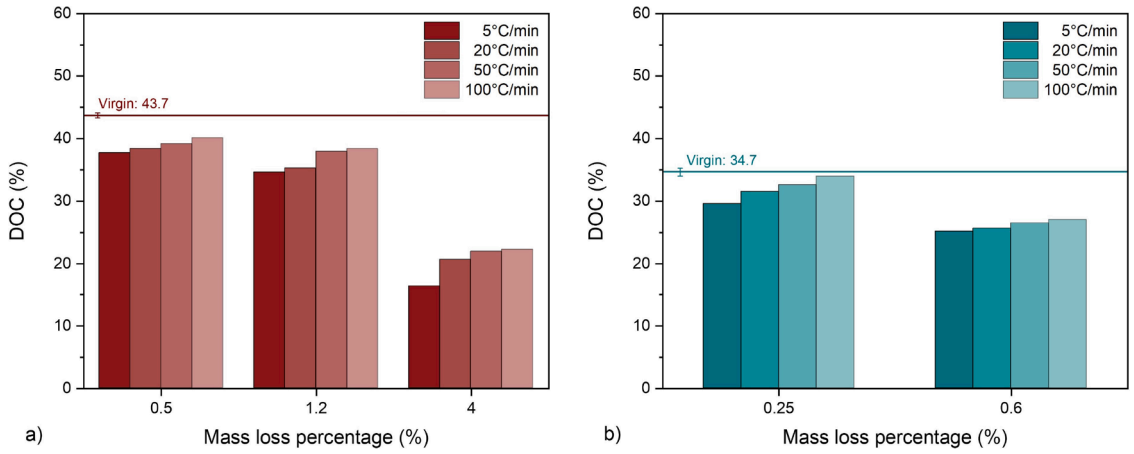

Fig. 19. DOC of a) PEEK and b) CF-PEEK as degradation progresses for the heating rates of 5, 20, 50 and 100 °C/min.

Table 3
T_m, T_g, T_c and DOC of virgin PEEK and of partially degraded PEEK when heated with heating rates of 5, 20, 50 and 100 °C/min.

Virgin PEEK	T_m: 342.7 °C		T_g: 145 °C		T_c: 298.05 °C		DOC: 43.7%	
Mass loss	5 °C/min				20 °C/min			
	T_m (°C)	T_g (°C)	T_c (°C)	DOC (%)	T_m (°C)	T_g (°C)	T_c (°C)	DOC (%)
0.5%	334.3	148.09	289.2	37.7	337	146.8	291.9	38.3
1.2%	328.7	149.6	283	34.6	332.8	148.3	288.6	35.3
4%	296.1	150.1	234.5	16.3	305	149.3	228.5	20.6
15%*	-	173.6	-	-	-	170.4	-	-
Mass loss	50 °C/min				100 °C/min			
	T_m (°C)	T_g (°C)	T_c (°C)	DOC (%)	T_m (°C)	T_g (°C)	T_c (°C)	DOC (%)
0.5%	337.02	146.3	292.2	39.1	339.17	147	292.2	40.1
1.2%	330.6	148.1	287.2	37.9	332.2	148.3	289.1	38.4
4%	296.9	149.2	231.1	21.9	307.4	150.6	284.6	22.2
15%*	-	173.7	-	-	-	160.9	-	-

*: Amorphous material.

4. Conclusions

This study provides a thorough investigation on the thermal degradation of PEEK and CF-PEEK in rapid high-temperature processing. Importantly, it establishes the 1711 cm^{-1} peak's intensity as a universal tool for detecting and characterising the extent of thermal degradation that occurs in the materials in the examined heating conditions. This can be a significant contribution to studies that aim to define the optimum process window of PEEK and CF-PEEK, since it provides a tool that can detect which processing conditions can reach high temperatures without inducing a severe thermal damage on PEEK and CF-PEEK in rapid high-temperature processing.

In addition, the analysis assesses the consequences of inducing a small-level thermal damage on the crystallinity content of PEEK and CF-PEEK. Therefore, it contributes to further defining their thermal limits in rapid high-temperature processing. Interestingly, a decomposition around 1% of the materials' PEEK content does not significantly affect PEEK's and CF-PEEK's DOC and could be considered tolerable as far as their crystallinity content is concerned. Furthermore, it is found that increased heating rates affect to a lesser extent the DOC of the materials.

Table 4
T_m, T_g, T_c and DOC of virgin CF-PEEK and of partially degraded CF-PEEK when heated with heating rates of 5, 20, 50 and 100 °C/min.

Virgin CF-PEEK	T_m: 340.3 °C		T_g: 140.3 °C		T_c: 292.3 °C		DOC: 34.7%	
Mass loss	5 °C/min				20 °C/min			
	T_m (°C)	T_g (°C)	T_c (°C)	DOC (%)	T_m (°C)	T_g (°C)	T_c (°C)	DOC (%)
0.25%	332.8	143.9	283.7	29.5	334.8	149.6	285.7	31.5
0.6%	316	152.7	257.5	25.1	318.5	150.6	255	25.6
1.7%*	-	186.7	-	-	-	157.8	-	-
6.7%*	-	**	-	-	-	**	-	-
Mass loss	50 °C/min				100 °C/min			
	T_m (°C)	T_g (°C)	T_c (°C)	DOC (%)	T_m (°C)	T_g (°C)	T_c (°C)	DOC (%)
0.25%	333.6	147.2	277.7	32.5	337.1	144.2	287	33.9
0.6%	321.3	155	257.8	26.5	331.6	149	273.3	27
1.7%*	-	182.2	-	-	-	157.6	-	-
6.7%*	-	**	-	-	-	**	-	-

*: Amorphous material.
**: Glass transition curve not detectable with the conducted DSC investigation.

When PEEK and CF-PEEK are heated upon degradation with faster heating rates their dwell time at temperatures above their melting point is significantly reduced. Hence, there is less time for the crosslinking mechanisms to take place which reduces the effect of thermal degradation on the DOC of the materials.

In summary, the developed thermal degradation assessment methodology of this study could be beneficial to several applications of PEEK and CF-PEEK where rapid high-temperature processing is involved. For instance, it could be used for optimising applications like induction welding, composite-metal laser joining and composites machining where the combination of reached temperatures and dwell time that is experienced locally at PEEK and CF-PEEK might not be easily captured and thermal degradation is one of the main damage mechanisms that could take place. Finally, the detection of the 1711 cm^{-1} peak's intensity could potentially be implemented as an in-line monitoring technique at the manufacturing of CF-PEEK composites. This would be an interesting application for further advancing PEEK's and CF-PEEK's industrial use and would further contribute to exploiting the outcomes of this study.

CRediT authorship contribution statement

Dimitrios Gaitanelis: Conceptualization, Methodology, Validation, Formal analysis, Investigation, Data curation, Writing – original draft, Writing – review & editing, Visualization. **Chris Worrall:** Conceptualization, Supervision, Project administration, Resources, Writing – review & editing. **Mihalis Kazilas:** Conceptualization, Supervision, Project administration, Resources, Writing – review & editing, Funding acquisition.

Declaration of Competing Interest

The authors declare that they have no known competing financial interests or personal relationships that could have appeared to influence the work reported in this paper.

Data availability

Data will be made available on request.

Acknowledgment

This publication was made possible by the sponsorship and support of TWI. The work was enabled through, and undertaken at, the National Structural Integrity Research Centre (NSIRC), a postgraduate engineering facility for industry-led research into structural integrity established and managed by TWI through a network of both national and international Universities.

References

[1] A. Pascual, M. Toma, P. Tsotra, M.C. Grob, On the stability of PEEK for short processing cycles at high temperatures and oxygen-containing atmosphere, Polym. Degrad. Stab. 165 (2019) 161–169, https://doi.org/10.1016/j.polymdegradstab.2019.04.025.
[2] G. Wypych, PEEK polyetheretherketone, in: G. Wypych (Ed.), Handbook of Polymers (Second Edition), ChemTec Publishing, 2016, pp. 366–370, https://doi.org/10.1016/B978-1-895198-92-8.50113-0.
[3] P. Patel, T.R. Hull, R.E. Lyon, S.I. Stoliarov, R.N. Walters, S. Crowley, N. Safronava, Investigation of the thermal decomposition and flammability of PEEK and its carbon and glass-fibre composites, Polym. Degrad. Stab. 96 (1) (2011) 12–22, https://doi.org/10.1016/j.polymdegradstab.2010.11.009.
[4] M. Kuo, C. Tsai, J. Huang, M. Chen, PEEK composites reinforced by nano-sized SiO2 and Al2O3 particulates, Mater. Chem. Phys. 90 (1) (2005) 185–195, https://doi.org/10.1016/j.matchemphys.2004.10.009.
[5] E.A.M. Hassan, D. Ge, L. Yang, J. Zhou, M. Liu, M. Yu, S. Zhu, Highly boosting the interlaminar shear strength of CF/PEEK composites via introduction of PEKK onto activated CF, Compos. Part A Appl. Sci.Manuf. 112 (2018) 155–160, https://doi.org/10.1016/j.compositesa.2018.05.029.
[6] H. Pérez-Martín, P. Mackenzie, A. Baidak, C.M. Ó Brádaigh, D. Ray, Crystallinity studies of PEKK and carbon fibre/PEKK composites: a review, Compos. Part B Eng. 223 (2021) 109–127, https://doi.org/10.1016/j.compositesb.2021.109127.
[7] E. Courvoisier, Y. Bicaba, X. Colin, Multi-scale and multi-technique analysis of the thermal degradation of poly(ether ether ketone), Polym. Degrad. Stab. 151 (2018) 65–79, https://doi.org/10.1016/j.polymdegradstab.2018.03.001.
[8] M. Martín, F. Rodríguez-Lence, A. Güemes, A. Fernández-López, L. Pérez-Maqueda, A. Perejón, On the determination of thermal degradation effects and detection techniques for thermoplastic composites obtained by automatic lamination, Compos. Part A Appl. Sci.Manuf. 111 (2018) 23–32, https://doi.org/10.1016/j.compositesa.2018.05.006.
[9] M. Day, J.D. Cooney, D.M. Wiles, The kinetics of the oxidative degradation of poly (aryl-ether-ether-ketone) (PEEK), Thermochim. Acta 147 (1) (1989) 189–197, https://doi.org/10.1016/0040-6031(89)85174-3.
[10] R. Phillips, T. Glauser, J.-A. Månanson, Thermal stability of PEEK/carbon fiber in air and its influence on consolidation, Polym. Compos. 18 (4) (1997) 500–508, https://doi.org/10.1002/pc.10302.
[11] M. Day, J.D. Cooney, D.M. Wiles, A kinetic study of the thermal decomposition of poly(aryl-ether-ether-ketone) (PEEK) in nitrogen, Polym. Eng. Sci. 29 (1) (1989) 19–22, https://doi.org/10.1002/pen.760290105.
[12] V. Mylläri, T.-P. Ruoko, J. Vuorinen, H. Lemmetyinen, Characterization of thermally aged polyetheretherketone fibres - mechanical, thermal, rheological and chemical property changes, Polym. Degrad. Stab. 120 (2015) 419–426, https://doi.org/10.1016/j.polymdegradstab.2015.08.003.
[13] P. Tsotra, M. Toma, A. Pascual, F. Schadt, C. Brauner, C. Dransfeld, Thermo-oxidative degradation of PEEK at high temperatures. Proceedings of the 18th European Conference on Composite Materials, ECCM18, Atans, Greece, 2018, pp. 25–28.
[14] G. Dolo, J. Férec, D. Cartié, Y. Grohens, G. Ausias, Model for thermal degradation of carbon fiber filled poly(ether ether ketone), Polym. Degrad. Stab. 143 (2017) 20–25, https://doi.org/10.1016/j.polymdegradstab.2017.06.006.
[15] T. Bayerl, M. Brzeski, M. Martínez-Tafalla, R. Schledjewski, P. Mitschang, Thermal degradation analysis of short-time heated polymers, J. Thermoplast. Compos. Mater. 28 (3) (2015) 390–414, https://doi.org/10.1177/0892705713486122.
[16] M. Bonmatin, F. Chabert, G. Bernhart, T. Djilali, Rheological and crystallization behaviors of low processing temperature poly(aryl ether ketone), J. Appl. Polym. Sci. 138 (47) (2021) 51402, https://doi.org/10.1002/app.51402.
[17] O. De Almeida, L. Feuillerat, J.-C. Fontanier, F. Schmidt, Determination of a degradation-induced limit for the consolidation of CF/PEEK composites using a thermo-kinetic viscosity model, Compos. Part A Appl. Sci.Manuf. 158 (2022) 106943, https://doi.org/10.1016/j.compositesa.2022.106943.

[18] T. Bayerl, M. Duhovic, P. Mitschang, D. Bhattacharyya, The heating of polymer composites by electromagnetic induction - a review, Compos. Part A Appl. Sci. Manuf. 57 (2014) 27–40, https://doi.org/10.1016/j.compositesa.2013.10.024.
[19] I.F. Villegas, P.V. Rubio, On avoiding thermal degradation during welding of high-performance thermoplastic composites to thermoset composites, Compos. Part A Appl. Sci.Manuf. 77 (2015) 172–180, https://doi.org/10.1016/j.compositesa.2015.07.002.
[20] X. Tan, J. Zhang, J. Shan, S. Yang, J. Ren, Characteristics and formation mechanism of porosities in CFRP during laser joining of CFRP and steel, Compos. Part B Eng. 70 (1) (2015) 35–43, https://doi.org/10.1016/j.compositesb.2014.10.023.
[21] C. Tan, J. Su, B. Zhu, X. Li, L. Wu, B. Chen, X. Song, J. Feng, Effect of scanning speed on laser joining of carbon fiber reinforced PEEK to titanium alloy, Opt. Laser Technol. 129 (2020) 106273, https://doi.org/10.1016/j.optlastec.2020.106273.
[22] J. Su, C. Tan, Z. Wu, L. Wu, X. Gong, B. Chen, X. Song, J. Feng, Influence of defocus distance on laser joining of CFRP to titanium alloy, Opt. Laser Technol. 124 (2020), https://doi.org/10.1016/j.optlastec.2019.106006.
[23] F. Lambiase, S. Genna, Laser-assisted direct joining of AISI304 stainless steel with polycarbonate sheets: thermal analysis, mechanical characterization, and bonds morphology, Opt. Laser Technol. 88 (2017) 205–214, https://doi.org/10.1016/j.optlastec.2016.09.028.
[24] K. Kerrigan, G.E. O'Donnell, On the relationship between cutting temperature and workpiece polymer degradation during CFRP edge trimming, Procedia CIRP 55 (2016) 170–175, https://doi.org/10.1016/j.procir.2016.08.041.5th CIRP Global Web Conference - Research and Innovation for Future Production (CIRPe 2016)
[25] G. Hou, B. Luo, K. Zhang, Y. Luo, H. Cheng, S. Cao, Y. Li, Investigation of high temperature effect on CFRP cutting mechanism based on a temperature controlled orthogonal cutting experiment, Compos. Struct. 268 (2021) 113967, https://doi.org/10.1016/j.compstruct.2021.113967.
[26] C. Leone, S. Genna, Heat affected zone extension in pulsed Nd:YAG laser cutting of CFRP, Compos. Part B Eng. 140 (2018) 174–182, https://doi.org/10.1016/j.compositesb.2017.12.028.
[27] C. Santiuste, J. Díaz-Álvarez, X. Soldani, H. Miguélez, Modelling thermal effects in machining of carbon fiber reinforced polymer composites, J. Reinf. Plast. Compos. 33 (8) (2014) 758–766, https://doi.org/10.1177/0731684413515956.
[28] F. Cepero-Mejías, J. Curiel-Sosa, A. Blázquez, T. Yu, K. Kerrigan, V. Phadnis, Review of recent developments and induced damage assessment in the modelling of the machining of long fibre reinforced polymer composites, Compos. Struct. 240 (2020), https://doi.org/10.1016/j.compstruct.2020.112006.
[29] Teijin, Tenax®Thermoplastics-E TPUD PEEK-HTS45. Product Data Sheet, 2022. https://www.teijincarbon.com/products/tenaxr-composites/tenaxr-thermoplastics
[30] A.G. Al Lafi, FTIR spectroscopic analysis of ion irradiated poly (ether ether ketone), Polym. Degrad. Stab. 105 (2014) 122–133, https://doi.org/10.1016/j.polymdegradstab.2014.04.005.
[31] D.J. Kemmish, J.N. Hay, The effect of physical ageing on the properties of amorphous PEEK, Polymer 26 (6) (1985) 905–912, https://doi.org/10.1016/0032-3861(85)90136-3.
[32] P. Cebe, S. Chung, S. Hong, Effect of thermal history on mechanical properties of polyetheretherketone below the glass transition temperature, J. Appl. Polym. Sci. 33 (2) (1987) 487–503, https://doi.org/10.1002/app.1987.070330217.Cited By 107
[33] S.-L. Gao, J.-K. Kim, Cooling rate influences in carbon fibre/PEEK composites. Part 1. Crystallinity and interface adhesion, Compos. Part A Appl. Sci.Manuf. 31 (6) (2000) 517–530, https://doi.org/10.1016/S1359-835X(00)00009-9.
[34] W.A. Pisani, M.S. Radue, S. Chinkanjanarot, B.A. Bednarcyk, E.J. Pineda, K. Waters, R. Pandey, J.A. King, G.M. Odegard, Multiscale modeling of PEEK using reactive molecular dynamics modeling and micromechanics, Polymer 163 (2019) 96–105, https://doi.org/10.1016/j.polymer.2018.12.052.
[35] A. Chanteli, A.K. Bandaru, D. Peeters, R.M. O'Higgins, P.M. Weaver, Influence of repass treatment on carbon fibre-reinforced PEEK composites manufactured using laser-assisted automatic tape placement, Compos. Struct. 248 (2020) 112539, https://doi.org/10.1016/j.compstruct.2020.112539.
[36] M. Day, T. Suprunchuk, J.D. Cooney, D.M. Wiles, Thermal degradation of poly (aryl-ether-ether-ketone) (PEEK): a differential scanning calorimetry study, J. Appl. Polym. Sci. 36 (5) (1988) 1097–1106, https://doi.org/10.1002/app.1988.070360510.
[37] M. Doumeng, L. Makhlouf, F. Berthet, O. Marsan, K. Delbé, J. Denape, F. Chabert, A comparative study of the crystallinity of polyetheretherketone by using density, DSC, XRD, and raman spectroscopy techniques, Polym. Test. 93 (2021) 106878, https://doi.org/10.1016/j.polymertesting.2020.106878.
[38] D. Blundell, B. Osborn, The morphology of poly(aryl-ether-ether-ketone), Polymer 24 (8) (1983) 953–958, https://doi.org/10.1016/0032-3861(83)90144-1.
[39] P. Patel, T.R. Hull, R.W. McCabe, D. Flath, J. Grasmeder, M. Percy, Mechanism of thermal decomposition of poly(ether ether ketone) (PEEK) from a review of decomposition studies, Polym. Degrad. Stab. 95 (5) (2010) 709–718, https://doi.org/10.1016/j.polymdegradstab.2010.01.024.
[40] M. Day, D. Sally, D. Wiles, Thermal degradation of poly(aryl-ether-ether-ketone): experimental evaluation of crosslinking reactions, J. Appl. Polym. Sci. 40 (9–10) (1990) 1615–1625, https://doi.org/10.1002/app.1990.070400917.
[41] J. Hay, D. Kemmish, Thermal decomposition of poly(aryl ether ketones), Polymer 28 (12) (1987) 2047–2051, https://doi.org/10.1016/0032-3861(87)90039-5.
[42] F. Yao, J. Zheng, M. Qi, W. Wang, Z. Qi, The thermal decomposition kinetics of poly(ether-ether-ketone) (PEEK) and its carbon fiber composite, Thermochim. Acta 183 (1991) 91–97, https://doi.org/10.1016/0040-6031(91)80448-R.
[43] S. Feih, A.P. Mouritz, Tensile properties of carbon fibres and carbon fibre-polymer composites in fire, Compos. Part A Appl. Sci.Manuf. 43 (5) (2012) 765–772, https://doi.org/10.1016/j.compositesa.2011.06.016.
[44] E. Kessler, R. Gadow, J. Straub, Basalt, glass and carbon fibers and their fiber reinforced polymer composites under thermal and mechanical load, AIMS Mater. Sci. 3 (4) (2016) 1561–1576, https://doi.org/10.3934/matersci.2016.4.1561.
[45] K.L. White, L. Jin, N. Ferrer, M. Wong, T. Bremner, H.-J. Sue, Rheological and thermal behaviors of commercial poly(aryletherketone)s, Polym. Eng. Sci. 53 (3) (2013) 651–661, https://doi.org/10.1002/pen.23309.
[46] A. Jonas, R. Legras, J.-P. Issi, Differential scanning calorimetry and infra-red crystallinity determinations of poly(aryl ether ether ketone), Polymer 32 (18) (1991) 3364–3370, https://doi.org/10.1016/0032-3861(91)90540-Y.
[47] H.X. Nguyen, H. Ishida, Molecular analysis of the melting behaviour of poly(aryl-ether-ether-ketone), Polymer 27 (9) (1986) 1400–1405, https://doi.org/10.1016/0032-3861(86)90041-8.
[48] H.X. Nguyen, H. Ishida, Molecular analysis of the crystallization behavior of poly (aryl-ether-ether-ketone), J. Polym. Sci. Part B Polym. Phys. 24 (5) (1986) 1079–1091, https://doi.org/10.1002/polb.1986.090240510.
[49] J.M. Chalmers, W.F. Gaskin, M.W. Mackenzie, Crystallinity in poly(aryl-ether-ketone) plaques studied by multiple internal reflection spectroscopy, Polym. Bull. 11 (1984) 433–435, https://doi.org/10.1007/BF00265483.
[50] K. Cole, Fourier transform infrared spectroscopic study of thermal degradation in films of poly(etheretherketone), Thermochim. Acta 211 (3) (1992) 209–228, https://doi.org/10.1016/0040-6031(92)87021-2.
[51] S.I. Kuroda, K. Terauchi, K. Nogami, I. Mita, Degradation of aromatic polymers - I. Rates of crosslinking and chain scission during thermal degradation of several soluble aromatic polymers, Eur. Polym. J. 25 (1) (1989) 1–7, https://doi.org/10.1016/0014-3057(89)90200-0.
[52] K. Cole, Fourier transform infra-red spectroscopic study of thermal degradation in poly(ether ether ketone)-carbon composites, Polymer 34 (4) (1992) 740–745, https://doi.org/10.1016/0032-3861(93)90357-G.
[53] N. Alsinani, M. Ghaedsharaf, L. Laberge Lebel, Effect of cooling temperature on deconsolidation and pulling forces in a thermoplastic pultrusion process, Compos. Part B Eng. 219 (2021) 108889, https://doi.org/10.1016/j.compositesb.2021.108889.
[54] J.J. Tierney, J. Gillespie Jr., Crystallization kinetics behavior of PEEK based composites exposed to high heating and cooling rates, Compos. Part A Appl. Sci. Manuf. 35 (5) (2004) 547–558, https://doi.org/10.1016/j.compositesa.2003.12.004.